AERE - R 6316

THIS DOCUMENT IS INTENDED FOR PUBLICATION IN THE OPEN LITERATURE. Until it is published, it may not be circulated, abstracted or referred to outside the organisations to which copies have been sent.

INDC-333

INDC(UK)-11/G

United Kingdom Atomic Energy Authority

RESEARCH GROUP

Report

THE RATIO OF THE ^{6}Li(n,α) TO ^{10}B(n,α) CROSS-SECTION FROM 10 eV TO 80 KeV AND RECOMMENDED VALUES OF THE ^{10}B(n,α) CROSS-SECTION

M. G. SOWERBY B. H. PATRICK

C. A. UTTLEY K. M. DIMENT

Nuclear Physics Division,

Atomic Energy Research Establishment,

Harwell, Berkshire.

1970

10

U.D.C.
546.34.02.6:539.172.4.816
546.27.02.10:539.172.4.816
539.172.4.816:546.34.02.6
539.171.02
539.172.4.816:546.27.02.10

THE RATIO OF THE ^{6}Li(n,α) TO ^{10}B(n,α) CROSS-SECTION FROM 10 eV TO 80 keV AND RECOMMENDED VALUES OF THE ^{10}B(n,α) CROSS-SECTION

by

M.G. Sowerby, B.H. Patrick, C.A. Uttley
and K.M. Diment

ABSTRACT

The ratio of the ^{6}Li(n,α) to ^{10}B(n,α) cross-sections has been measured in the energy range 10 eV to 80 keV using the Harwell linear accelerator time-of-flight spectrometer. By combining the ratio data with values of the ^{6}Li(n,α) cross-section deduced from an accurate total cross-section measurement, the ^{10}B(n,α) cross-section has been obtained. This is compared with the cross-section determined from recent measurements of the total and scattering cross-sections of ^{10}B. All these data have been fitted by an analytical expression, the form of which has been derived from theoretical arguments, using a least squares fitting procedure and it is found that up to 200 keV, the ^{10}B(n,α) cross-section $\sigma_{n\alpha}(^{10}B)$ is given by

$$\sigma_{n\alpha}(^{10}B) = \frac{13.837}{\sqrt{E}} - 0.312 - 1.014 \times 10^{-2}\sqrt{E} + \frac{2.809 \times 10^{5}}{\sqrt{E}\,[(170.3-E)^{2} + 2.243 \times 10^{4}]} \text{ barns}$$

where E is in keV.

Nuclear Physics Division,
U.K.A.E.A. Research Group,
Atomic Energy Research Establishment,
HARWELL.

March 1970

HL.70/1170 (C17)
HMD.

CONTENTS

TABLES

ILLUSTRATIONS

1. Introduction

In the course of some experiments by Patrick et al.[1] to measure eta, alpha and the neutron cross-sections of ^{239}Pu in the energy range 10 eV to 30 keV using the Harwell linear accelerator time-of-flight spectrometer, the relative incident neutron flux was measured using detectors based on the $^{6}Li(n,\alpha)$ and $^{10}B(n,\alpha)$ reactions. It was assumed that, over the energy range of interest, the energy dependence of these reaction cross-sections was adequately represented by a $1/\sqrt{E}$ law but the neutron spectra obtained from the two detectors were inconsistent at the higher energies. It is important to establish the energy dependence of these cross-sections accurately since they are the most useful reactions with which to measure neutron flux below 100 keV. The data from the two detectors can be used to obtain accurate values of the ratio of the $^{6}Li(n,\alpha)$ to $^{10}B(n,\alpha)$ cross-sections as a function of neutron energy and have been used as a basis to investigate the energy dependence of the $^{10}B(n,\alpha)$ cross-section. This has been done by combining the ratio measurement with the absorption cross-section of ^{6}Li deduced from an accurate measurement of the total cross-section over a wide energy range (70 eV to 7 MeV) and calculations of the scattering cross-section of ^{6}Li.

In this paper the measurements of the neutron flux are described and the ratio of the cross-sections obtained. A brief outline of the determination of the absorption cross-section of ^{6}Li is given and a comparison is made between the $^{10}B(n,\alpha)$ cross-section obtained by this method and that determined from recent measurements of the total and scattering cross-sections of ^{10}B.

2. Experimental Method

Two measurements covering the energy regions 10 eV to 2 keV and 50 eV to 80 keV have been made on the 45 MeV Harwell Linear Accelerator time-of-flight spectrometer. These experiments will be referred to as the low energy and high energy experiments respectively. In both experiments the relative incident neutron spectrum was measured with a 0.3 cm thick Li glass scintillator (NE 905). The glass was 6.35 cm diameter and was mounted 5.25 cm away from the photomultiplier to reduce the effect of neutrons scattered in the photomultiplier on the efficiency of the detector. In the low energy experiment the spectrum was also measured with a 5 cm diameter, copper-walled, $^{10}BF_3$ counter (20th Century Electronics Type 40 EB 70/50). In the high energy experiment the second spectrum measurement was made with a "Boron plug" detector[2] which consists of an array of NaI crystals which detect the 478 keV γ-rays from the $^{10}B(n,\alpha_1\gamma)$ reaction produced in a sample of ^{10}B in the neutron beam. The ^{10}B sample had a total mass of 3.38 gms and was 7.6 cms in diameter. The details of the experiments are given in Table 1.

The time-of-flight of each event was recorded on a 1 inch magnetic tape recorder fitted with a six word input buffer so that several events could be recorded per machine cycle. The number of time channels was 8192. A PDP-4 computer was used to analyse the events into time spectra. The backgrounds were measured by the use of resonance filters.

If, for a given detector, $N(E)$ is the number of counts at energy E in the interval ΔE, then this is related to the efficiency of the detector $\varepsilon(E)$ and the incident neutron flux $\phi(E)$ by the expression

$$N(E) = \varepsilon(E)\phi(E) \qquad \text{..... (1)}$$

For a detector of uniform thickness

$$\varepsilon(E) = k[1 - T(E)] \frac{n\sigma_\alpha(E)}{\log_e \{1/T(E)\}} S(E) \qquad \text{..... (2)}$$

where n is the number of ^6Li or ^{10}B atoms per cm^2; $\sigma_\alpha(E)$ is the appropriate (n,α) cross-section; $S(E)$ is a factor which allows for the effect of multiple scattering in the detector and surrounding material; k is a constant which allows for the fact that not all the (n,α) events are accepted because of solid angle, pulse height analysis, etc. - in the case of the "Boron plug" detector, k also includes the ^{10}B branching ratio because only ~93% of the (n,α) events are of the $(n,\alpha_1\gamma)$ type and in the analysis of the results k has a small energy dependence because of the slight change in the branching ratio with energy at the upper end of the energy region covered by the measurements; $T(E)$ is the neutron transmission of the detector and is given by

$$T(E) = A \exp[-n\sigma_\alpha(E)] \qquad \text{..... (3)}$$

where $A = \exp[-\{\sum_i n_i\sigma_i(E) + n\sigma_s(E)\}]$, n_i being the number of atoms per cm^2 of the i^{th} constituent of the detector other than ^6Li or ^{10}B, $\sigma_i(E)$ its total neutron cross-section and $\sigma_s(E)$ the neutron scattering cross section of the ^6Li or ^{10}B. Both detectors are sufficiently "thin" (small n-value) such that the energy dependence of σ_i and σ_s have a negligible effect on the value of A which can be taken to be a constant.

If for one of the experiments, $N_L(E)$ and $N_B(E)$ are the number of counts in ΔE for the lithium and boron detectors, then from equations (1), (2) and (3) the ratio between these counts can be expressed as

$$\frac{N_L(E)}{N_B(E)} = \frac{k_L}{k_B}\ \frac{n_L\sigma_{\alpha L}(E)}{n_B\sigma_{\alpha B}(E)}\ \frac{S_L(E)}{S_B(E)}\ \frac{F_L(E)}{F_B(E)} \qquad \text{..... (4)}$$

where $F(E) = \dfrac{1 - A\exp[-n\sigma_\alpha(E)]}{\log_e(1/A) + n\sigma_\alpha(E)}$, the suffices L and B referring to the lithium and boron detectors respectively.

For "thin" detectors both S(E) and F(E) approach unity and the measured ratio $N_L(E)/N_B(E)$ gives a direct determination of the ratio of the (n,α) cross-sections provided $k_L n_L$ and $k_B n_B$ are known. Now in the case of the detectors used in these measurements, both F(E) and S(E) do not differ greatly from unity and it can be shown that their values are insensitive to small changes in the cross-sections. Hence only an approximate value of σ_α at any energy is needed to obtain accurate values of F(E) and S(E). Thus by calculating F(E) and S(E) using approximate values for σ_α the ratio $N_L(E)/N_B(E)$ enables the ratio of the cross-sections to be determined. The ratio $N_L(E)/N_B(E)$ is normalised at low energies (~10 eV) where both the (n,α) cross-sections are well known, so that it is not necessary to know the values of k and the values of n are only required to obtain F(E) and S(E), these again being insensitive to the exact n values.

3. Efficiency of Detectors

The probability of a neutron producing an alpha particle in the Li glass detector has been calculated using two Monte Carlo codes assuming that σ_α for ^{6}Li varies as $1/\sqrt{E}$. In the first calculation, which used a code of Lynn and Moxon[3], it was assumed that the neutrons all interacted on the axis of the disc while in the second, which was performed by Hart[4] using the GEM code[5], the neutron beam was assumed to be 5 cm diameter. In order to obtain accurate values of A and n the neutron transmission of the glass was measured as a function of neutron energy (equation (3)). The values obtained were $A = 0.932 \pm 0.003$ and $n = 0.004433 \pm 0.000129$ atoms per barn. Table 2 gives typical values of the calculated probabilities and the values of S(E) and it can be seen that the results of the two calculations agree to better than 2%. The results of calculation (2) have been used for the analysis of the present experiment.

The calculations of the multiple scattering correction for the "Boron plug" were made using the code of Lynn and Moxon and typical results are given in Table 3. It was assumed in the calculation that the boron was uniformly spread over the surface of the disc. It can be seen that S(E) is near unity in this case.

The efficiency of the BF_3 counter, which was mounted with its axis perpendicular to the neutron beam, was calculated by Hart using the GEM code assuming there are no neutron resonances in copper. The results of this calculation, which are given in Table 4, agree within ± 0.1% with an analytical calculation made assuming that the counter had no walls.

4. Results

The results of the experiments are given in Table 5 and plotted in Fig. 1. The low energy experiment has been normalised to a value of 0.2450 in the energy range 10 to 20 eV. This value was chosen because Diment[6] and Uttley and Diment[7] have deduced from their total cross-section measurements on ^{10}B and ^{6}Li that the low energy absorption cross-sections are given by $^{610.3}/\sqrt{E(eV)}$ barns and $^{149.5}/\sqrt{E(eV)}$ barns respectively. Extrapolating to 0.0253 eV these expressions give values of 3839 ± 20 and 940 ± 4 barns respectively which agree with the values of 3836 ± 7 and 945 barns given in the review by Spaepen[8]. The high energy experiment was normalised to the low energy one in the region of 1 keV. Corrections have been applied to the data to allow for the variation of the ^{10}B branching ratio above 10 keV.

The errors in the measured ratios, which are shown on a few points in Fig. 1, are mainly systematic and are listed in Tables 6 and 7. The error in the normalising value of 0.245 is considered to be ± 0.5% and statistics increase the low energy experiment normalisation error to 0.6%. The error in normalisation of the high energy experiment is ± 1.0%. By normalising the experiments the magnitudes of the systematic errors are reduced in the vicinity of the normalising regions.

There are three groups of data at approximately 570 eV, 1.3 keV and 2.8 keV which are high because of inadequate corrections. The first two are due to the fact that allowance has not been made in the Monte Carlo calculations for the effects of the 577 eV resonance in the cross-section of the copper of the BF_3 counter and the 1.3 keV resonance in the cross-section of cerium present in the Li glass scintillator. The high points at 2.8 keV are due to the scattering of neutrons from the sodium in the glass face of the photomultiplier even although it is mounted 5.25 cms behind the Li glass scintillator in the neutron beam. The observed increase in counts agrees with a calculation which also shows that the scattering is negligible at all other energies.

There is only one other direct measurement of the ratio of the $^{6}Li(n,\alpha)$ and $^{10}B(n,\alpha)$ cross-sections which can be compared with the present experiment. Bergman and Shapiro[9] using the lead slowing-down spectrometer measured the ratio in the energy range 8 eV to 25 keV. The results agree well with the present experiment below

3 keV but are lower at higher energies by up to 3%. The discrepancy is probably not significant.

5. Discussion

Having obtained values for the ratio of the (n,α) cross-sections of ^{6}Li and ^{10}B, we can calculate the cross-section for one if we know the values of the other. We choose to take ^{6}Li(n,α) as the known cross-section and deduce the ^{10}B(n,α) cross-section for the following reasons. In the neighbourhood of the neutron binding energy, the level density of ^{7}Li is much less than that of ^{11}B and consequently there is less chance of weak levels contributing to the ^{6}Li cross-section than to that of ^{10}B. The first known level in ^{7}Li above the neutron binding energy lies at 247 keV whereas in ^{11}B there are two known levels within the first 150 keV. Over the range of neutron energies considered here, (n,α) and (n,γ) are the only possible reactions in ^{6}Li whereas in ^{10}B, (n,α), (n,γ), (n,p) and (n,t) are all possible. The ^{6}Li(n,γ) cross-section has been measured at thermal energies by Bartholomew and Campion[10] as 28 ± 8 mb which is negligible compared to the (n,α) cross-section. The information on (n,γ), (n,p) and (n,t) reactions for ^{10}B is sparse and is summarised by Gubernator and Moret[11]. The (n,γ) cross-section for the production of the 4.444 MeV γ-ray in ^{11}B is 0.5 ± 0.2 barns at thermal energies. Using the branching ratio data of Thomas et al[12] this implies that the total (n,γ) cross-section is not greater than 1 barn, which is negligible compared with the absorption cross-section of 3836 barns. A measurement at 230 keV by Biggerstaff[13] observed zero cross-section with an upper limit of 10 mb which is less than 1% of the absorption cross-section. As far as the ^{10}B(n,p) cross-section is concerned, Crespi and Cairo[14] found that the thermal value is less than 7 mb, while Mooring et al[15] concluded from the measurements of Eggler et al[16] that the average cross-section from 10 keV to 500 keV is less than 30 mb (i.e. less than ~2% of the absorption cross-section). The ^{10}B(n,t) cross-section has been measured by Klein and Mooring[17] at 230 keV and an upper limit of 60 mb is given. It is not surprising that the cross-sections for (n,p) and (n,t) are small since the Q-values are low and the charged particles have to be emitted with angular momentum $l \geqslant 2$ for s-wave neutron absorption. It has therefore been assumed in this paper that all absorption cross-sections other than (n,α) are zero. As a result of these comments, we feel that there is a greater possibility of being able to obtain accurate values of the ^{6}Li cross-section, rather than that of ^{10}B, in particular by using total cross-section measurements; we shall now proceed along these lines.

Uttley and Diment[7] have recently measured the ^{6}Li total cross-section over the energy range 70 eV to 7 MeV, the details of which will be published later. However, some of the results will be used here. The data have been analysed to give the resonance parameters of the 247 keV resonance. Since this resonance is produced by p-wave neutrons, it is superimposed on an s-wave contribution which is conveniently found by analysing the data below 5 keV where the contribution from the resonance is negligible. In this region the total cross-section is found to be described by the expression

$$\sigma_{nT}(\mathrm{Li}) = {}^{149.5}/_{\sqrt{E(\mathrm{eV})}} + 0.696 \text{ barns} \qquad \ldots\ldots (5)$$

There have been two other recent measurements of the ^{6}Li total cross-section. The first, by Hibdon and Mooring[18] in the energy range 10 to 1236 keV, gives results which are in very good agreement with those of Uttley and Diment. The second, by Farrell and Pineo[19] who measured over the energy range 50 to 650 keV, is, in general, in good agreement with Uttley and Diment except on the peak of the resonance where Farrell and Pineo obtain values ~0.4 barn lower. However, we are interested here in the (n,α) cross-section below 100 keV only where the three experiments agree.

The second term in Equation (5) is essentially the low energy scattering cross-section and is in very good agreement with the preliminary value of 0.70 barn obtained in a direct measurement by Asami and Moxon[20]. The first term in Equation (5) is the well known $^1/_{\sqrt{E}}$ term and is essentially entirely due to the (n,α) reaction since the capture cross-section is very small. It is worth noting that the resonance parameters of Uttley and Diment predict a scattering cross-section over the resonance which is in very good agreement with the experimental measurements of Lane et al[21], thus adding weight to the assumption that the analysis is correct.

The absorption cross-section has been obtained from the total cross-section data by two methods. In the first, an exact calculation of the scattering cross-section was made, an account of which is given by Diment and Uttley[22]. This smooth calculated scattering cross-section was subtracted from the measured total cross-section and the results are plotted in Fig. 2. In the second method, the absorption cross-section was calculated and the resulting smooth curve is also shown in Fig. 2 where it can be seen that the agreement between the two sets of results is extremely good in the region of interest.

Fig. 3 shows the values of the ^{6}Li(n,α) cross-section as measured by various experiments in the energy range 10 to 150 keV. Also shown is the smooth calculated curve of

Uttley and Diment along with their fit to the total cross-section which is included for comparison purposes. It is immediately clear that the (n,α) cross-section values at 10.7 and 12 keV, measured by Cox and Pontet[23] are much too high since they are essentially equal to the total cross-section and we have seen that the scattering cross-section is ~0.7 barn. The value at 22 keV is also clearly too large as the difference between it and the total cross-section is less than half of the scattering cross-section. It thus appears that the data of Cox and Pontet are probably in error and can be neglected.

Of the other sets of data between 10 and 150 keV, those of Barry[24] and Bame and Cubitt[25] have been measured relative to the ^{235}U fission cross-section. The lowest energy point of Barry at 25 keV was normalised to the Sb-Be source measurement of the ^{235}U fission cross-section made by Perkin et al[26]. High resolution time-of-flight measurements of this cross-section by Patrick et al[27] show that there is considerable structure in this energy region and the cross-section averaged over the source energy spectrum may be as much as 10% higher than that in the region of 25 keV. The results of Bame and Cubitt used here have been renormalised (see Bergström et al[28]) to take account of later measurements of the ^{235}U fission cross-section. However, because of the presence of structure, it is felt that measurements based on the ^{235}U fission cross-section are subject to uncertainties of at least 5%. In the experiment of Bame and Cubitt, a ^{6}LiI(Eu) crystal was used as a combined ^{6}Li sample and detector. No corrections were made for the effects of multiple scattering in the crystal, although some were made for the presence of the crystal container and photomultiplier, and so it might be expected that their results will be too high.

In Fig. 3, the absorption cross-section values of Schwarz et al[29] appear to be in reasonable agreement with the calculated values. However, this is not surprising since, in the region below 40 keV, the data were normalised to a $1/\sqrt{E}$ extrapolation from the thermal cross-section. Thus these results cannot be used to indicate deviations from a ($1/\sqrt{E}$ + resonance) dependence. The single energy measurement of Condé et al[30] at 100 keV obtained 0.64 ± 0.02 barn in very good agreement with the calculated value of 0.65 barn.

In view of the above comments, we feel that at present, the values of the (n,α) cross-section obtained from the fit to the total cross-section are the best available set. Since the total cross-section shows no sign of structure below the 247 keV resonance, there seems to be no reason for believing that the absorption cross-section is as high as the measured values indicate. Farrell and Pineo also obtained parameters for the 247 keV resonance and deduced the absorption cross-section over the resonance and down to 40 keV. The difference between the two calculations is never more than 5% but since Uttley and Diment had the advantage of data for their analysis extending well into the $^1/\sqrt{E}$ region, it is likely that it will be the more accurate.

We can now find the $^{10}B(n,\alpha)$ cross-section using the results of the ratio measurement together with the $^{6}Li(n,\alpha)$ cross-section values obtained by Uttley and Diment. We have chosen to use the absorption cross-section found by subtracting the calculated smooth scattering cross-section from the measured total cross-section rather than use the calculated absorption cross-section for the following reasons. We shall want to compare the $^{10}B(n,\alpha)$ cross-section deduced from these data with that obtained from measurements of the total and scattering cross-sections. All the data are then as close as possible to being the actual experimentally measured averages containing similar statistical fluctuations rather than the results of a smooth fit. Clearly, since the $^{6}Li(n,\alpha)$ cross-section data obtained by the two different methods are in very good agreement, there will be no difference in the results and conclusions whichever set is used.

In obtaining the $^{10}B(n,\alpha)$ cross-section from the ratio and $^{6}Li(n,\alpha)$ data, the data were averaged over suitable energy intervals, weighting each point in the time-of-flight measurements by its energy width, and in order to show deviations from a $^1/\sqrt{E}$ behaviour more clearly, the resulting data have been divided by $^{19.30}/\sqrt{E(keV)}$ averaged over the same energy intervals. The relative cross-section thus found is plotted in Fig. 4 with estimated errors being shown on a few representative points. Also shown are the absorption cross-section values of Mooring et al(15) and the results obtained by subtracting the scattering cross-section data of Asami and Moxon(31) from the total cross-section data of Diment. Above 100 keV, the scattering cross-section data of Mooring et al were used since the data of Asami and Moxon did not extend into this region. The data of Bogart and Nichols(32) and Nellis et al(33) have been neglected because of their relatively large errors.

It can be seen from Fig. 4 that the agreement between the various sets of data is very good. It is clear that the $^{10}B(n,\alpha)$ cross-section does not vary as $^1/\sqrt{E}$ as the relative cross-section falls below this level reaching a minimum in the region of 25 keV where the cross-section is ~4% below the $^1/\sqrt{E}$ level. Because of this deviation and the large energy spread of their normalisation point at 30 keV, we have not included the data of Macklin and Gibbons(34) in Fig. 4. Above this energy the relative cross-section passes through a resonance and peaks at ~150 keV. That there appears to be a resonance in this region is quite reasonable since the energy level compilations of Ajzenberg-Selove and Lauritsen[35] show a level in ^{11}B, which decays by α-emission, at 140 ± 35 keV above the neutron separation energy.

Although it is usually assumed that the $^{10}B(n,\alpha)$ and $^{6}Li(n,\alpha)$ cross-sections follow a $^{1}/_{\sqrt{E}}$ law until the vicinity of the first resonance above thermal energy, Shapiro[36] has shown that the cross-section σ cannot be strictly proportional to $^{1}/_{\sqrt{E}}$ but must have the form

$$\sigma = {}^{A}/_{\sqrt{E}} + \Delta\sigma + \beta\sqrt{E} + \gamma E^{3/2} + \ldots \qquad \ldots\ldots (6)$$

where A, $\Delta\sigma$, β and γ are constants. $\Delta\sigma$ depends on the square of the thermal cross-section and upon the fraction of that cross-section due to resonances of spin $J = I + {}^{1}/2$ and $J = I - {}^{1}/2$, where I is the spin of the target nucleus. The values of $\Delta\sigma$ are small and always negative, and only cause significant deviations from the $^{1}/_{\sqrt{E}}$ law above neutron energies of a few keV. β and the higher terms are usually considered to be small except in the vicinity of resonances. In regions where Equation (6) is valid, β is positive if the levels responsible for the low energy cross-section lie above the neutron binding energy and negative if they lie below. Using the Shapiro expression for $\Delta\sigma$, it can be shown that for ^{6}Li, $\Delta\sigma \sim -0.02$ barn. However, the value for ^{10}B is expected to be much larger since the thermal cross-section is about four times that of ^{6}Li and Bergman and Shapiro deduced a value of -0.40 ± 0.03 barn from a measurement of the ratio of the (n,α) cross-sections of ^{6}Li and ^{10}B. Thus the deviation of the data from a $^{1}/_{\sqrt{E}}$ behaviour as shown in Fig. 4 is indicative of the presence of the $\Delta\sigma$ term and possibly also of a significant value of β.

The measured energy dependence of the cross-section suggests that it may be possible to fit the data with an expression which contains the first three terms of the Shapiro expansion (Equation (6)) and an s-wave resonance in the region of 150 keV. We write the $^{10}B(n,\alpha)$ cross-section $\sigma_{n\alpha}(^{10}B)$ as

$$\sigma_{n\alpha}(^{10}B) = {}^{19.30}/_{\sqrt{E}} + \Delta\sigma + \beta\sqrt{E} + \frac{K}{\sqrt{E}}\left[\frac{1}{(E - E_0)^2 + \frac{\Gamma^2}{4}} - \frac{1}{E_0{}^2 + \frac{\Gamma^2}{4}}\right] \text{barns} \quad \ldots (7)$$

where $\Delta\sigma$, β and K are constants, E is the neutron energy in keV, E_0 is the resonance energy in keV and Γ is the total width of the resonance in keV. It has been assumed that

$\Gamma_\alpha >> \Gamma_n$ and hence $\Gamma_\alpha \sim \Gamma$. The second term in the square brackets is included to remove the $^1/\sqrt{E}$ tail of the resonance term since it is already included in the term $^{19.30}/\sqrt{E}$. It should be noted that if resonance interference effects are present then the energy dependence of the interference terms will be similar to Equation (6) but with the addition of a term proportional to E.

Dividing Equation (7) by $^{19.30}/\sqrt{E}$ we obtain the following expression for the relative cross-section

$$\frac{\sigma_{n\alpha}(^{10}B)}{^{19.30}/\sqrt{E}} = 1 + A\sqrt{E} + BE + C\left[\frac{1}{(E-E_o)^2 + \frac{\Gamma^2}{4}} - \frac{1}{E_o{}^2 + \frac{\Gamma^2}{4}}\right] \qquad \ldots\ldots (8)$$

where A, B and C are constants.

A programme was written to fit this expression to all the data plotted in Fig. 4 by adjusting the quantities A, B, C, E_o and Γ to minimise the sum of the squares of the differences, equal weight being given to all the data points. It can be seen from the curve drawn through the data in Fig. 4, which is the result of this fit, that it is not necessary to consider more than the first three terms in the Shapiro expansion. The resonance energy is found to be 170.3 keV and the width Γ = 299.5 keV. The value of $\Delta\sigma$ obtained is -0.31 barn and the best fit is obtained with $\beta = -1.01 \times 10^{-2}$ barns.(keV)$^{-1/2}$. If common terms in Equation (7) are collected together and the expression simplified, then the cross-section $\sigma_{n\alpha}$ of ^{10}B is given by:

$$\sigma_{n\alpha}(^{10}B) = {}^{13.837}/\sqrt{E} - 0.312 - 1.014 \times 10^{-2}\sqrt{E} + \frac{2.809 \times 10^5}{\sqrt{E}\,[(170.3 - E)^2 + 2.243 \times 10^4]} \text{ barns} \qquad \ldots\ldots (9)$$

where E is in keV. Table 8 gives the accuracy of the cross-section as calculated from this expression.

While the above expression is a good description of the energy dependence of the cross-section, great care must be taken in interpreting the meaning of the various parameters. It is quite likely that other expressions can be found which give equally good fits. The s-wave resonance included in the present analysis accounts for 28% of the low energy cross-section, but, if the resonance is attributed to p-waves, an equally good fit is obtained. The presence of other small resonances would certainly destroy the validity of this analysis and it is to be noted that there is a level in ^{11}B at

6 ± 10 keV above the neutron separation energy. The data tend to suggest the existence of a resonance in the region of 40 keV but the inclusion of another resonance is not justified by the accuracy of the data. If we take Equation (9) seriously, the negative sign of β would suggest that, in the absence of resonance interference effects, the levels responsible for the low energy $^{10}B(n,\alpha)$ cross-section lie below the neutron binding energy, which is opposite to the conclusion reached by Bergman and Shapiro. However, these authors did not allow for the contribution of the 247 keV resonance in the $^{6}Li(n,\alpha)$ cross-section. Since this contributes about 5% of the cross-section at 25 keV, the upper limit of their experiment, this omission makes their analysis invalid.

6. Conclusions

Summarising, the ratio of the (n,α) cross-sections of ^{6}Li and ^{10}B has been measured from 10 eV to 80 keV with an accuracy ranging from 1.5 to 3.5%. It has been shown that if these results are combined with the $^{6}Li(n,\alpha)$ cross-section values deduced by Uttley and Diment from fits to their measured total cross-section, the resulting values of the $^{10}B(n,\alpha)$ cross-section are in very good agreement with those derived or measured in other ways. The cross-section has been written in terms of an analytic expression, the form of which has been derived from theoretical arguments. This expression has been fitted to all the cross-section data and the result is given by Equation (9). We conclude that Equation (9) describes the $^{10}B(n,\alpha)$ cross-section up to 200 keV within an accuracy ranging from 1% up to 1 keV, 2% at 10 keV, 2% at 10 keV, 3% at 100 keV and 5% at 200 keV and it is recommended that this equation be used where neutron fluxes are determined with detectors based on the $^{10}B(n,\alpha)$ reaction.

It has been shown that the $^{10}B(n,\alpha)$ cross-section is now known to a considerably higher accuracy than previously since the results of three independent measurements agree so well. However, in the case of $^{6}Li(n,\alpha)$, although we believe that the Uttley and Diment calculated cross-section is probably equally accurate, the agreement between the various measurements is much poorer, as indicated in Fig. 3. Thus, at present, the $^{10}B(n,\alpha)$ cross-section is the better known one but in deciding whether ^{6}Li or ^{10}B should be considered as the primary standard, the following points should be noted. Several reactions besides (n,α) are energetically possible in ^{10}B whereas capture is the only other one possible in ^{6}Li. Although these cross-sections are known to be small, it is clearly desirable for a primary standard to have as few competing reactions as possible so that use can be made of accurate total cross-section data and scattering cross-section measurements to obtain the appropriate cross-section used in the flux determinations.

The possible presence of resonances in the ^{10}B cross-sections below 150 keV means that the $^{10}B(n,\alpha)$ cross-section is by no means an ideal case for use as a standard.

Clearly, as a result of the greater accuracy with which the $^{10}B(n,\alpha)$ cross-section is known, it will continue to be used very widely in the determination of neutron fluxes. Nevertheless, in view of the statements above, we suggest that the $^{6}Li(n,\alpha)$ cross-section be considered as the primary standard in the region below 100 keV.

Acknowledgements

The authors are grateful to Dr. E.R. Rae for his continued interest in this work. The assistance of Mr. M.G. Schomberg during the measurements and in the analysis is greatly appreciated. We are also indebted to Drs. D.B. Gayther, M.S. Coates and Mr. J.S. Story for helpful discussions and to Dr. W. Hart for the Monte Carlo calculations of efficiencies.

References

(1) B.H. Patrick, M.G. Schomberg, M.G. Sowerby and J.E. Jolly, Proc. Conf. on Nuclear Data for Reactors, IAEA Vienna, Vol. II, p.117 (1967).

(2) E.R. Rae and E.M. Bowey, Proc. Phys. Soc. A66, 1073 (1953).

(3) J.E. Lynn and M.C. Moxon, private communication.

(4) W. Hart, private communication.

(5) P.J. Hemmings, UKAEA Report AHSB(S)R105.

(6) K.M. Diment, UKAEA Report AERE - R 5224.

(7) C.A. Uttley and K.M. Diment, to be published.

(8) J. Spaepen, Proc. Conf. on Nuclear Data for Reactors, IAEA Vienna, Vol. I, p.241 (1967).

(9) A.A. Bergman and F.L. Shapiro, Soviet Physics JETP 13, 895 (1961).

(10) G.A. Bartholomew and P.J. Campion, Can. J. Phys. 35, 1347 (1957).

(11) K. Gubernator and H. Moret, Euratom report EUR 3950 e.

(12) G.E. Thomas, D.E. Blatchey and L.M. Bollinger, Nuc. Inst. and Meth. 56, 325 (1967).

(13) J.A. Biggerstaff, Oak Ridge report ORNL-TM-1271, p.8.

(14) M.B. Crespi and A.E. Cairo, J. Inorg. Nuc. Chem. 3, 248 (1956).

(15) F.P. Mooring, J.E. Monohan and C.M. Huddleston, Nuc. Phys. 82, 16 (1966).

(16) C. Eggler, D.J. Hughes and C. Huddleston, Phys. Rev. 74, 1239 (1948).

(17) P.D. Klein and F.P. Mooring, cited in Ref. (15).

(18) C.T. Hibdon and F.P. Mooring, Proc. Conf. on Neutron Cross Sections and Technology, Washington, p.159 (1968).

(19) J.A. Farrell and W.F.E. Pineo, Proc. Conf. on Neutron Cross Sections and Technology, Washington, p.153 (1968).

(20) A. Asami and M.C. Moxon, private communication.

(21) R.O. Lane, A. Elwyn, F.P. Mooring and A. Langsdorf, Bull. Am. Phys. Soc. 12, 87 (1967).

(22) K.M. Diment and C.A. Uttley, Nuclear Physics Division Progress Reports AERE - PR/NP 15, p.12 and AERE - PR/NP 16, p.3.

(23) S.A. Cox and F.R. Pontet, J. Nucl. Energy, 21, 271 (1967).

(24) J.F. Barry, Proc. Conf. on Neutron Cross Sections and Technology, Washington, p.763 (1966).

(25) S.J. Bame and R.L. Cubbitt, Phys. Rev. 114, 1580 (1959).

(26) J.L. Perkin, P.H. White, P. Fieldhouse, E.J. Axton, P. Cross and J.C. Robertson, J. Nucl. Energy 19, 423 (1965).

(27) B.H. Patrick, M.G. Sowerby and M.G. Schomberg, UKAEA Report AERE - R 6350.

(28) A. Bergström, S. Schwarz, L.G. Strömberg and L. Wallin, Neutron Data Compilation Centre, Paris, Report CCDN-NW 3.

(29) S. Schwarz, L.G. Strömberg and A. Bergström, Nuc. Phys. 63, 593 (1965).

(30) H. Condé, S. Schwarz and N. Starfelt, Arkiv Fysik 29, 45 (1965).

(31) A. Asami and M.C. Moxon, UKAEA Report AERE - R 5980.

(32) D. Bogart and L.L. Nichols, Nuc. Phys. A125, 463 (1969).

(33) D.O. Nellis, W.E. Tucker and I.L. Morgan, to be published.

(34) R.L. Macklin and J.H. Gibbons, Phys. Rev. 165, 1147 (1968).

(35) F. Ajzenberg-Selove and T. Lauritsen, Nuc. Phys. A114, 1 (1968).

(36) F.L. Shapiro, Soviet Physics JETP 7, 1132 (1958).

TABLE I

Experimental Details

Experiment	Low Energy	Low Energy	High Energy	High Energy
Spectrum detector	0.3 cm thick Li glass scintillator	5 cm diameter $^{10}BF_3$ counter	0.3 cm Li glass scintillator	"Boron Plug" Detector
Reaction detected	^{6}Li(n,α)	^{10}B(n,α_0) + ^{10}B(n,$\alpha_1\gamma$)	^{6}Li(n,α)	^{10}B(n,$\alpha_1\gamma$)
Neutron Pulse Width (unmoderated) (nS)	220	220	220	220
Timing Channel Width (nS)	125	125	125	125
Flight path length (m)	34.9	35.97	97.55	97.55
Nominal Resolution (nS/m)	7.2	7.0	2.5	2.5
Permanent "black" filters	Na + Boron	Na + Boron	Al + Boron	Al + Boron
Resonance Filters for background measurement	Mn, Mo, Ta	Mn, Mo, Ta	Mn, Au	Mn, Au

TABLE 2

Efficiency of 0.3 cm thick Li glass scintillator

Neutron Energy (eV)	Monte Carlo (1) (ε/k)	Monte Carlo (2) (ε/k)	S(E) (1)	S(E) (2)
10	0.1986	0.1973	1.103	1.096
100	0.06903	0.0682	1.133	1.119
1C00	0.02259	0.02224	1.151	1.133
10000	0.007272	0.007134	1.158	1.136
30000	0.004161	0.004086	1.156	1.135

TABLE 3

Efficiency of 3.38 grm ^{10}B plug

Neutron Energy (eV)	Efficiency (ε/k)	S(E)
10	0.4960	1.008
100	0.1955	1.014
1000	0.06653	1.018
10000	0.02174	1.022
30000	0.01272	1.023

TABLE 4

Efficiency of 5 cm diameter BF_3 counter

Neutron Energy (eV)	Efficiency (ε/k)	S(E)
10	0.01796	1.006
31	0.01034	1.009
103	0.005696	1.012
310	0.003278	1.015
1030	0.001815	1.018

TABLE 5

Experimental values and errors of the ratio of the $^{6}Li(n,\alpha)$ and $^{10}B(n,\alpha)$ cross-sections. Each ratio is an average over an energy interval from E to E+0.15E and the energy E' is given by E' = E+0.075E

Low Energy Experiment			High Energy Experiment		
Energy E' (eV)	Ratio $\frac{\sigma_{n\alpha}(^{6}Li)}{\sigma_{n\alpha}(^{10}B)}$	Error in Ratio	Energy E' (eV)	Ratio $\frac{\sigma_{n\alpha}(^{6}Li)}{\sigma_{n\alpha}(^{10}B)}$	Error in Ratio
10.0	0.2440	22×10^{-4}	52	0.2469	53×10^{-4}
11.4	0.2461	22 "	59	0.2426	50 "
13.2	0.2478	22 "	68	0.2455	47 "
15.1	0.2455	22 "	78	0.2458	44 "
17.4	0.2456	23 "	90	0.2445	42 "
20.0	0.2451	23 "	104	0.2453	40 "
23	0.2438	23 "	119	0.2446	39 "
26	0.2441	24 "	137	0.2451	39 "
30	0.2446	24 "	158	0.2433	38 "
35	0.2436	25 "	182	0.2460	38 "
40	0.2449	26 "	209	0.2449	37 "
46	0.2439	26 "	240	0.2453	35 "
53	0.2410	26 "	276	0.2456	34 "
61	0.2452	27 "	317	0.2453	34 "
70	0.2422	27 "	365	0.2453	33 "
81	0.2438	28 "	420	0.2438	33 "
93	0.2433	29 "	483	0.2454	32 "
107	0.2412	29 "	555	0.2454	31 "
123	0.2432	30 "	639	0.2468	31 "
142	0.2421	32 "	734	0.2475	30 "
163	0.2433	32 "	845	0.2465	28 "
187	0.2445	33 "	971	0.2468	27 "
215	0.2448	33 "	1120	0.2481	27 "
248	0.2420	34 "	1280	0.2520*	–
285	0.2432	34 "	1480	0.2480	28 "
328	0.2446	34 "	1700	0.2475	28 "
377	0.2424	35 "	1950	0.2498	30 "
433	0.2425	35 "	2250	0.2501	30 "
498	0.2448	36 "	2580	0.2536*	–
573	0.2553*	–	2970	0.2539*	–
659	0.2436	35 "	3420	0.2504	30 "
758	0.2448	35 "	3930	0.2518	30 "
871	0.2464	37 "	4520	0.2543	30 "
1002	0.2500	37 "	5200	0.2532	30 "
1152	0.2454	37 "	5980	0.2542	30 "
1325	0.2526*	–	6870	0.2527	30 "
			7900	0.2542	30 "
			9090	0.2535	30 "
			10500	0.2563	31 "
			12000	0.2555	31 "
			13800	0.2559	31 "
			15900	0.2589	31 "
			18300	0.2563	31 "
			21000	0.2591	31 "
			24200	0.2593	31 "
			27800	0.2617	31 "
			32000	0.2606	31 "
			56000	0.2794	67 "
			64000	0.2829	68 "
			74000	0.2883	69 "

*Results affected by resonances in structural materials of detectors and are neglected in fitting of data (see text).

TABLE 6

Errors in cross-section ratios for low energy experiment

Energy (eV)	% error due to background uncertainties	% error due to BF_3 counter efficiency	% error due to normalisation	% error Li glass efficiency		% Error Statistics	Total Error (%)
				Errors in n and A	Errors in S(E)		
10	0.0	0.0	0.6	0.0	0.0	0.6	0.9
30	0.5	0.1	0.6	0.1	0.4	0.6	1.0
100	0.7	0.3	0.6	0.2	0.5	0.6	1.2
300	0.8	0.4	0.6	0.2	0.7	0.6	1.4
1000	0.7	0.5	0.6	0.2	0.8	0.6	1.5

TABLE 7

Errors in cross-section ratios for high energy experiment

Energy (eV)	% error due to background uncertainties	% error due to normalisation	% Error Li Glass Efficiency		% Error Boron Plug Efficiency		% Error Statistics	Total Error (%)
			Errors in n and A	Errors in S(E)	Uniformity n and A	Errors in S(E)		
50	1.5	1.0	0.0	0.3	1.0	0.2	0.5	2.2
100	0.9	1.0	0.0	0.2	0.8	0.2	0.5	1.7
300	0.3	1.0	0.0	0.1	0.4	0.1	0.5	1.4
1000	0.0	1.0	0.0	0.0	0.0	0.0	0.5	1.1
3000	0.4	1.0	0.0	0.1	0.1	0.1	0.5	1.2
10000	0.4	1.0	0.0	0.2	0.2	0.2	0.5	1.2
30000	0.4	1.0	0.0	0.2	0.3	0.2	0.4	1.2
60000	0.4	1.0	0.0	0.2	0.3	0.2	0.5	2.4*

*Includes a 2% error due to uncertainties in neutron energy.

TABLE 8

The uncertainty in the $^{10}B(n,\alpha)$ cross-section given by Equation (9)

Energy (keV)	Uncertainty ± %
≤ 1	1
10	2
100	3
200	5

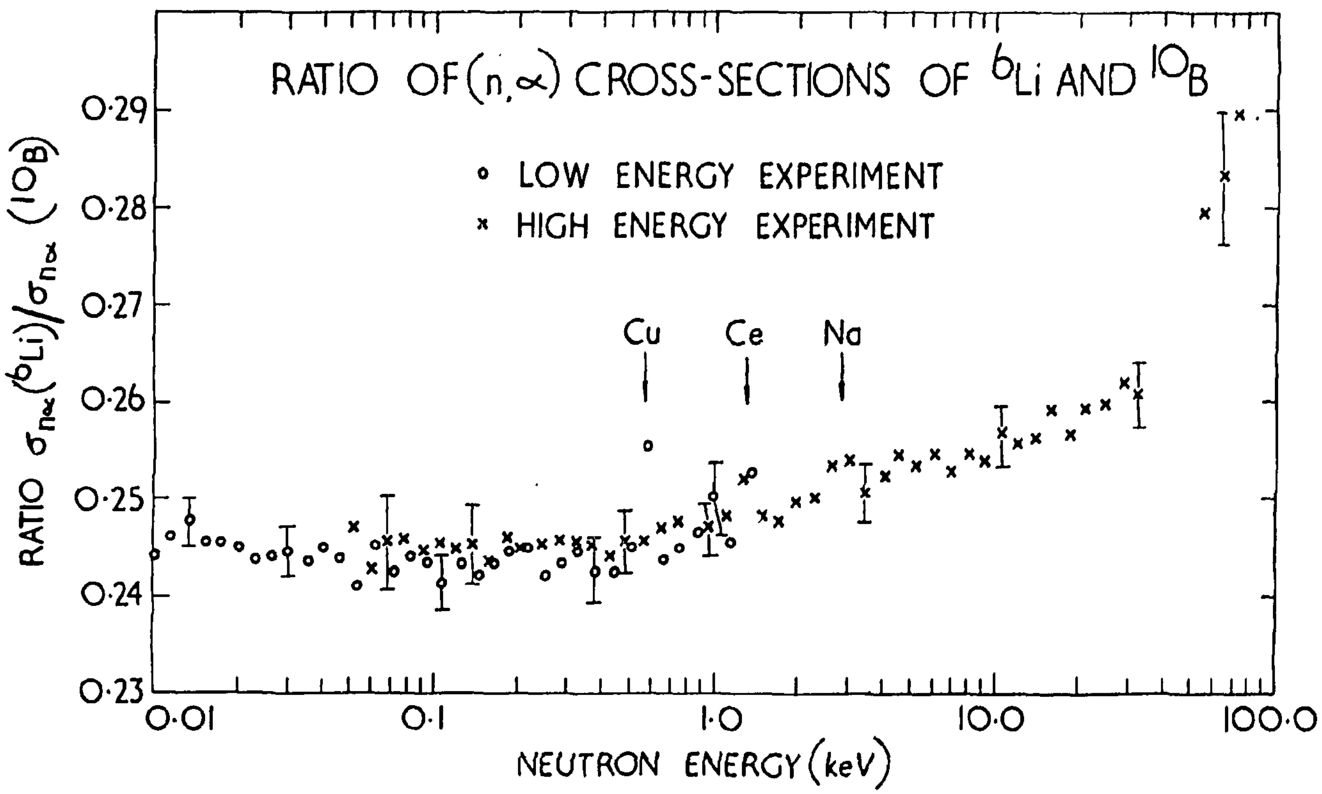

AERE - R 6316 Fig. 1

The measured ratio of the ^{6}Li(n,α) and ^{10}B(n,α) cross-sections. The arrows labelled Cu and Ce indicate the positions of resonances in the cross-sections of the copper walls of the BF_3 counter and of the cerium present as a constituent of the lithium glass scintillator. The arrow marked Na indicates the position of the 2.85 keV resonance in sodium, where the effect of neutrons scattered from the glass of the photomultiplier is observed.

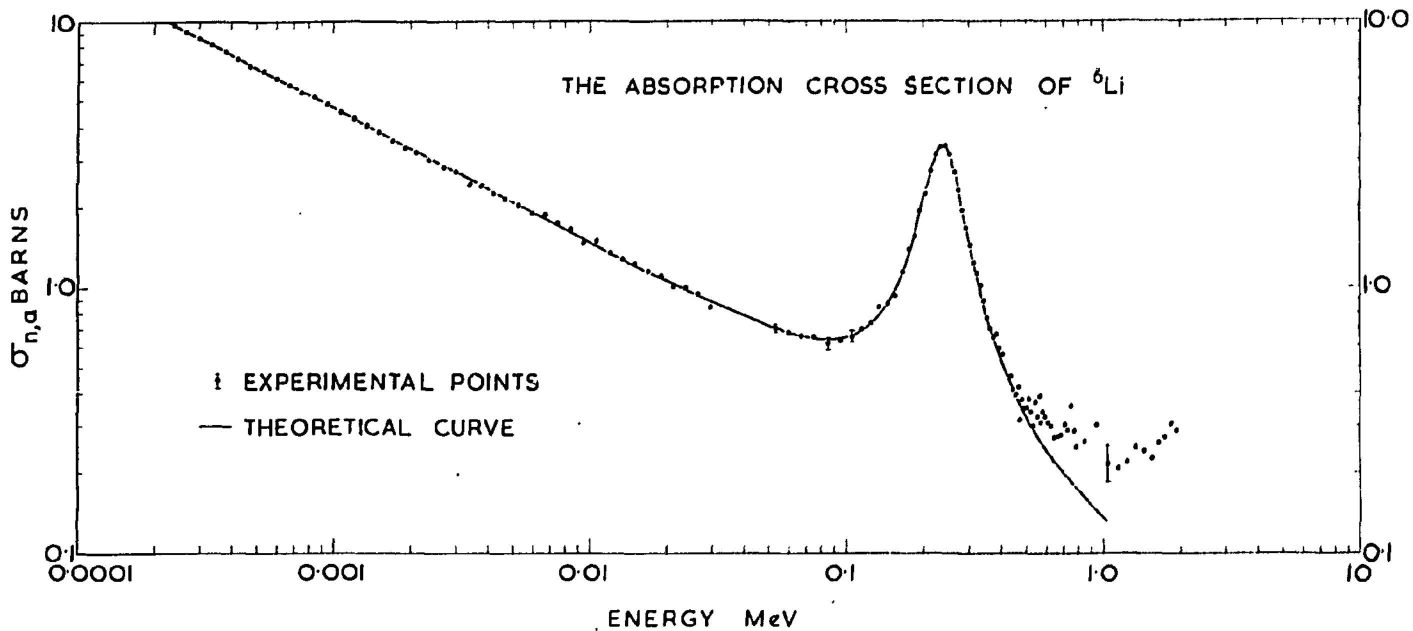

AERE - R 6316 Fig. 2

The absorption cross-section of ^{6}Li from 200 eV to 2 MeV. The points are the values obtained by subtracting the calculated scattering cross-section from the measured total cross-section. The curve represents the calculated absorption cross-section.

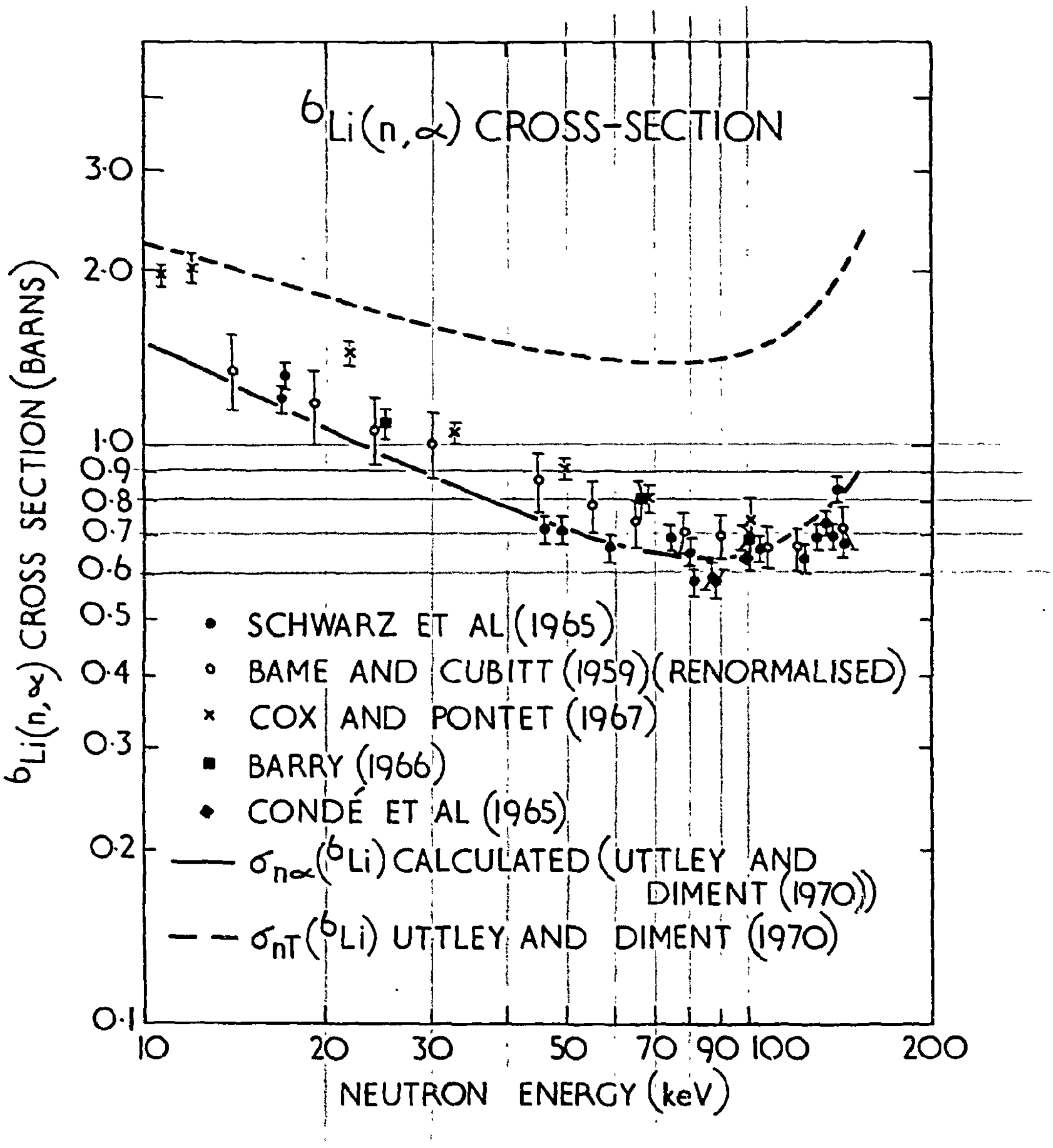

AERE - R 6316 Fig. 3

The ^{6}Li(n,α) cross-section from 10 to 150 keV.

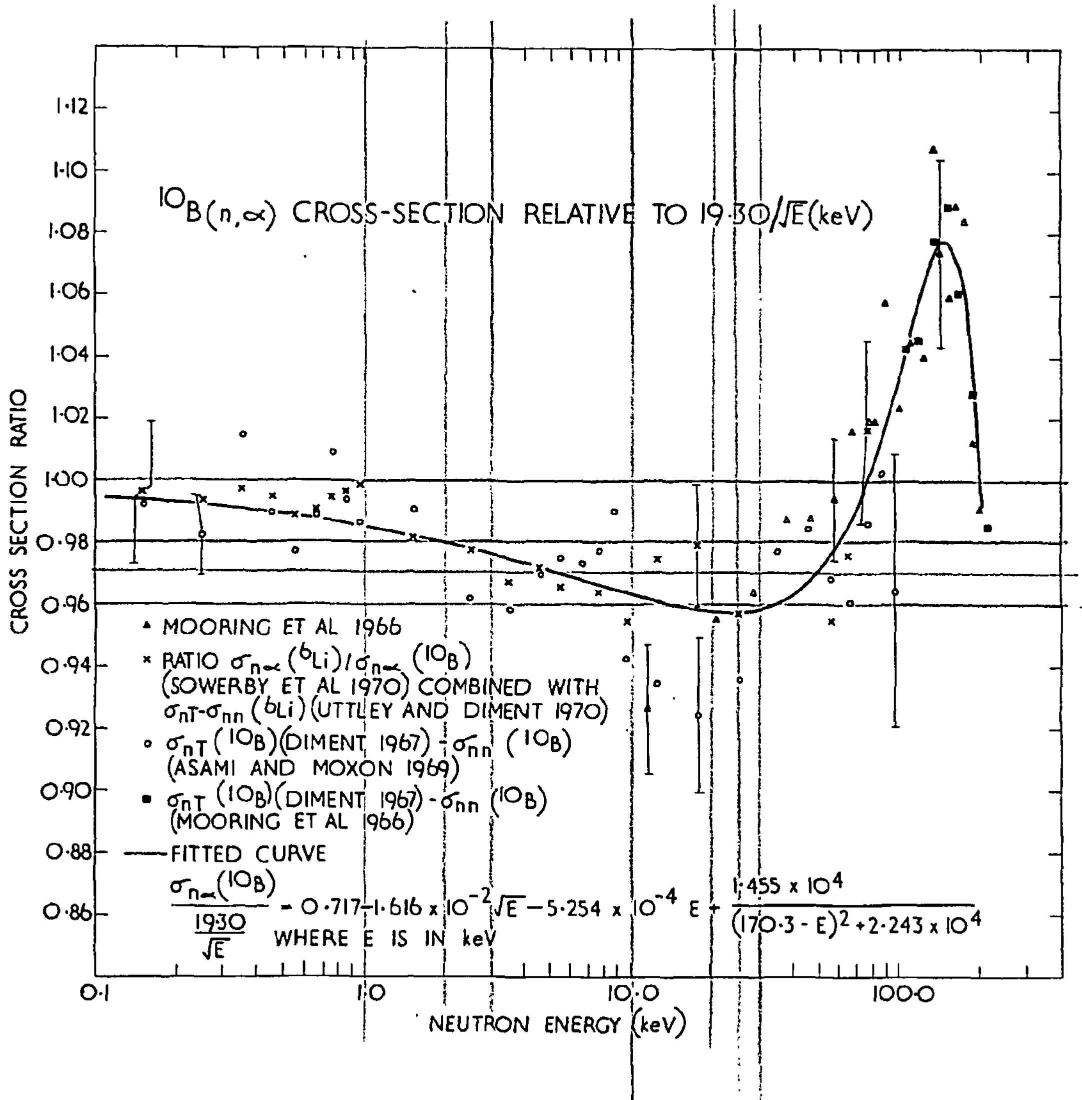

AERE - R 6316 Fig. 4

The ^{10}B(n,α) cross-section relative to $19.30/\sqrt{E(\text{keV})}$ from 100 eV to 200 keV.